Tunnelling and Underground Space Technology 26 (2011) 139–145

Contents lists available at ScienceDirect

Tunnelling and Underground Space Technology

journal homepage: www.elsevier.com/locate/tust

An experimental study of the effect of local contact loss on the earth pressure distribution on existing tunnel linings

C. Leung, M.A. Meguid *

Department of Civil Engineering and Applied Mechanics, McGill University, 817 Sherbrooke Street West, Montreal, Quebec, Canada H3A 2K6

ARTICLE INFO

Article history:
Received 20 December 2009
Received in revised form 17 July 2010
Accepted 24 August 2010
Available online 22 September 2010

Keywords:
Tunnel lining
Earth pressure
Soil-structure interaction
Physical model
Contact loss

ABSTRACT

This study presents the results of the experimental investigation that has been conducted to examine the effect of local contact loss between a tunnel lining and the surrounding ground on the earth pressure distribution acting on the tunnel liner. An experimental setup has been designed using a mechanically adjustable tunnel model to simulate the initial lining pressure that results from shield tunnelling. A local separation between the lining and the surrounding soil was introduced at different locations around the tunnel and the changes in contact pressure were measured. Results indicated significant changes in earth pressure in the close vicinity of the area that has experienced the contact loss. The changes in earth pressure differed greatly depending on the location of the induced separation. When located at the invert and haunches results showed an increase in pressure by about 28%, whereas a pressure decrease of about 75% was measured immediately above the separated section when located at the springline. The above results suggest that the presence of a small lining area that is not in direct contact with the surrounding ground can have a significant impact on the performance of the tunnel lining.

1. Introduction

Tunnel linings are usually designed to support part or complete overburden pressure depending on the geometric and geological conditions of the tunnel and the surrounding ground (Terzaghi, 1943). In calculating the lining load, full contact is generally assumed between the lining and the supported soil throughout the service life of the tunnel. However, local support loss may develop around tunnels due to several reasons including improper grouting and erosion of the supporting soils. Erosion voids initiate around tunnel linings in the form of weakened zones caused by the inflow of groundwater carrying fine particles through existing cracks (Asakura and Kojima, 2003). The resulting contact loss can lead to re-distribution of the earth pressure acting on the lining and, consequently, changes the internal forces in the lining structure. Fine grained soils such as sand and silt have been identified among the most susceptible supporting material to erosion (MacDonald and Zhao, 2001). The Highway & Rail Transit Tunnel Maintenance & Rehabilitation Manual (US Department of Transportation, 2006) highlighted that "fine soil particles can be carried through cracks with water, creating void behind the liner, which can cause settlement of surrounding structures and/or cause eccentric loading on tunnels that can lead to unforeseen stresses". A schematic of a tunnel lining experiencing local contact loss is shown in Fig. 1.

Several case histories involving lining damage due to soil erosion have been reported in the literature. Among the recent cases, two sewage tunnels and one water tunnel in the US in addition to a transportation tunnel in Japan (ITA, 1991). In all cases, tunnels were built in silty or sandy soils and experienced a loss of soil support around the springlines and invert of the tunnel lining. It has been observed that support loss at the tunnel invert causes differential settlement which leads to circumferential cracking whereas support loss at the sides causes ovalisation and longitudinal cracking of the lining. Non-destructive testing (NDT) has been used to detect the presence of voids around existing tunnels. Davis et al. (2005) employed impulse radar signals to examine a section of a water supply tunnel in Buenos Aires, Argentina. The results indicated the presence of voids near the springline of the tunnel lining. Early detection has assisted in taking the proper repair measures to prevent lining distress and cracking. Helfrich (1997) studied the failure of a 0.3 m diameter sewer pipe made of vitrified clay and buried at a depth of 3 m below ground surface. Sections of the pipe settled about 50 mm leading to significant distress in the pipe structure. Major sections of the pipe had to eventually be replaced with new bedding layers underneath the pipe. Talesnick and Baker (1999) reported the failure of a large diameter (1.2 m) composite pipe due to the development of a 200 mm void beneath the invert that extended 300 m along the pipe. These examples illustrate the possible disastrous consequences of the support loss around existing buried structures.

Very few studies have been devoted to investigate the effect of void formation around tunnels and buried pipes on the performance

* Corresponding author. Tel.: +1 514 398 1537; fax: +1 514 398 7361.
E-mail address: mohamed.meguid@mcgill.ca (M.A. Meguid).

0886-7798/$ - see front matter © 2010 Elsevier Ltd. All rights reserved.
doi:10.1016/j.tust.2010.08.003

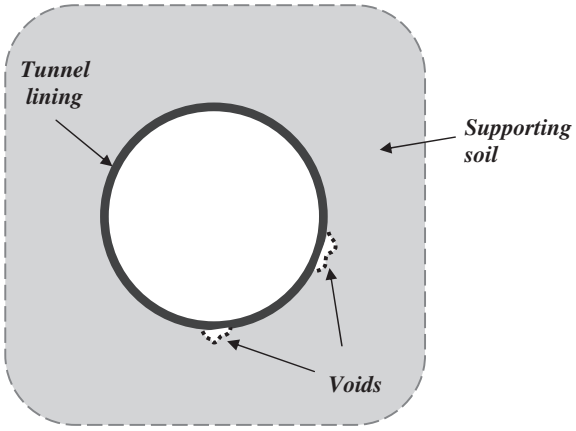

Fig. 1. Contact loss around tunnel lining.

of these structures. Tan and Moore (2007) investigated numerically the effect of void formation on the performance of buried rigid pipes. The influence of both the void size and location (e.g. springline and invert) on the stresses and bending moments developing in the pipe wall was investigated. Results of an elastic model showed that the presence of a void at the springline leads to an increase in the extreme fiber stresses and the bending moments at all critical locations: crown, springlines and invert. The rate of increase is controlled by the growth of the void in contact with the rigid pipe. Extending the model to include the shear failure effect resulted in stresses and moments higher than those reported in the elastic analysis. Meguid and Dang (2009) conducted a numerical study on the effect of erosion void development around an existing tunnel on the circumferential stresses in the tunnel lining. A series of elasto-plastic finite element analysis was carried out to investigate the effect of different parameters (e.g., flexibility ratio, coefficient of earth pressure at rest and void size) on thrust forces and bending moments in the lining. When the void was located at the springline, bending moment significantly increased. The presence of erosion void at the lining invert was found to reduce the bending moments causing reversal in the sign of the moment as the void size increased.

The above studies contributed to the understanding of how the presence of voids would affect the performance of an existing rigid or flexible tunnel lining. However, experimental studies are needed to confirm the above findings and provide additional information about the effect of void formation and local support loss on the earth pressure distribution acting on a buried structure. The objective of this study is to experimentally investigate the effects of local contact loss around an existing tunnel on the earth pressure distribution on the tunnel lining. The experimental setup and detailed components of the model tunnel are first described. Local separation is introduced at three different locations around the tunnel, namely, springline, invert and haunch. The measured earth pressure results are then summarized and compared with the initial earth pressure values.

2. Experimental setup

Several physical models have been developed by researchers to study the ground response to tunnelling in soft ground including the trap door method (e.g. Park et al., 1999), preinstalled tubes with vinyl facing (e.g. Chambon and Corte, 1994), mechanically adjustable linings (Lee and Yoo, 2006) and miniature tunnel boring machines (Nomoto et al., 1999). These methods are described in more details elsewhere (Meguid et al., 2008). Among these methods, the mechanically adjustable lining system has been proven to be successful in approximately simulating the 2D soil movement associated with the gap-closure around a tunnel lining installed in cohesionless soil. A series of experiments were conducted in this study to examine the changes in earth pressure acting on a tunnel lining subjected to local contact loss. A description of the different components and the experimental procedure is given below.

2.1. Strong box

The testing facility has been designed such that the entire model was contained in a rigid steel tank. As illustrated in Fig. 2, the tank is approximately 1410 mm wide, 1270 mm high and 300 mm thick with a 12 mm plexiglass face. Both the front and rear sides were reinforced using three 100 mm HSS sections. The internal steel sides of the tank were painted and lined with plastic sheets to reduce friction between the sand and the sides of the tank. On the front and rear sides, a hole of 152 mm in diameter was drilled. The hole size was chosen to be larger than the outer diameter of the tunnel to ensure that the tunnel rests directly on the sand. The location of the opening was selected to minimize the influence of the tank rigid boundaries on the measured earth pressure and to ensure sufficient overburden pressure over the tunnel with cover to diameter (C/D) ratio of 2. This was achieved by placing the lateral boundaries at a distance of approximately four times the tunnel diameter (4.2D) measured from its circumference. The tank rigid base was located at a distance of 2.2D below the tunnel invert to represent the case of a tunnel installed in soft ground overlying bedrock.

2.2. Tunnel model

One of the challenges of the experimental setup was to develop a suitable mechanism to simulate the local contact loss between the pipe wall and the surrounding medium while recording the corresponding earth pressure changes around the pipe. This was achieved by designing and machining a segmented lining composed of six curved segments sliced from a cold drawn steel pipe (114 mm in diameter and 610 mm in length) and six aluminum strips. To hold the different circular sectors of the pipe, six stainless steel U-shape grooved pieces were used. The different pipe sectors were assembled such that the segments tightly fit between the lips of the holding pieces. The U-shaped pieces were hinged to a 25 mm

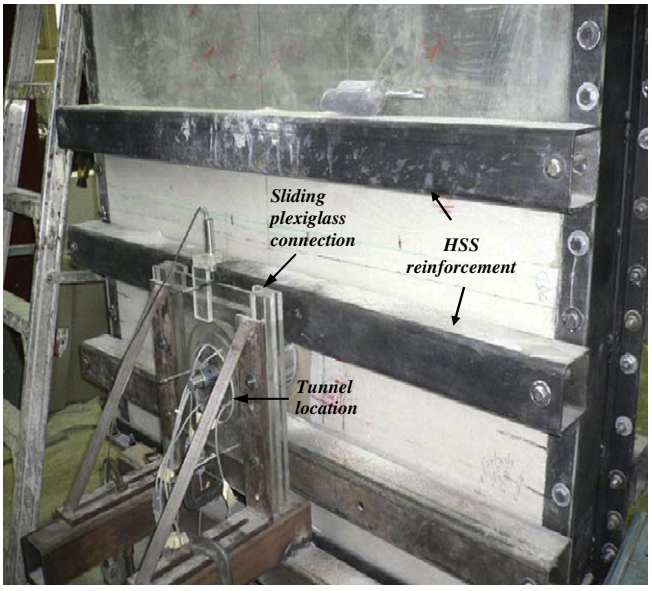

Fig. 2. Test setup.

hexagonal nut screwed at each side to a threaded rod passing along the pipe length. The movement of the nuts allows a 3 mm shrinkage of the outer diameter of the pipe. The aluminum shims were placed such that one of the ends is bolted to one of the pipe segment while the other end is left to slide freely over the adjacent segment. Two of the shims were fixed whereas the remaining four strips were removable. The small gaps between the shims and the lining were sealed with clear silicone caulking so that the fine sand particles could not enter and damage the sensors. Fig. 3a and b show parts of the model tunnel as well as its inner mechanics. Under full expansion condition, the tunnel outer diameter is 150 mm.

To simulate the local contact loss, a small retractable window was installed on one of the thick lining plates. This small window measured 0.4 inch (10 mm) by 10 inches (254 mm). This area would equate to about 1.5% of the lining circumference or a void angle of 5.1° as compared to Meguid and Dang (2009) and Tan and Moore (2007), respectively. The retraction of the window was a miniature version of the tunnel contraction mechanism, the difference being that in the case of the window; only one small plate needs be retracted. Otherwise the action included two small threaded rods of opposing directions that were connected together at the center of the plate by a custom made coupling nut. To move the window, a threaded rod was turned, causing the hinges to move towards the coupling nut and therefore the window moves inward. The window was calibrated to retract exactly 1.5 mm per full (360°) rotation with a maximum retraction of 3.5 mm. The tunnel was designed so that the window could be positioned at the springline, invert and at haunch. Fig. 4 shows the internal details of the retractable window.

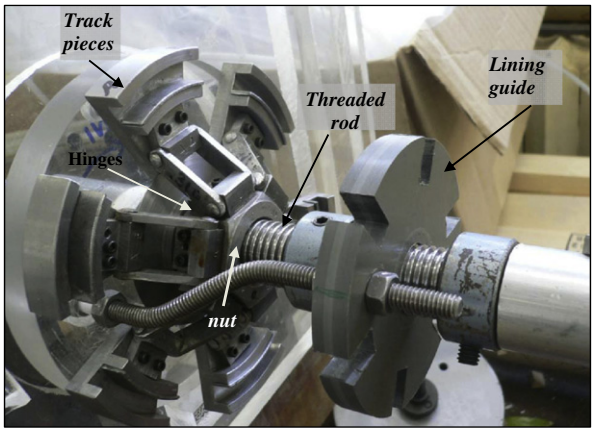

(a) Inner tunnel parts without lining

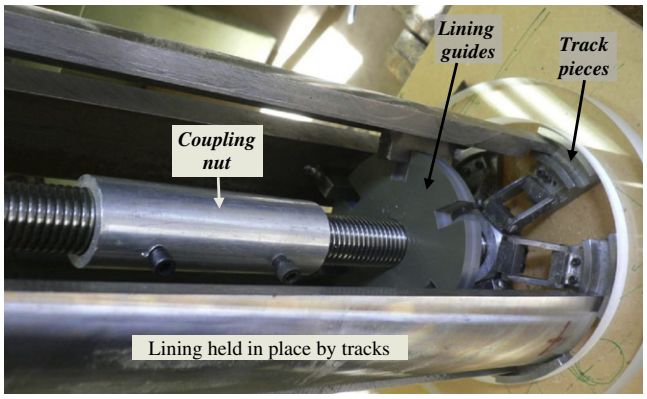

(b) lining segments partially installed

Fig. 3. The mechanically adjustable tunnel: (a) inner tunnel parts without lining and (b) lining segments partially installed.

2.3. Instrumentation

To measure the earth pressure distribution, the lining was instrumented with eight sensors connected to a data acquisition system. Four of the sensors (Scaime AR load cells) have maximum capacity of 1200 g with accuracy of ±0.02% while the remaining ones (Futek LBB load cells) have maximum capacity of 250 g with accuracy of ±0.05%. All sensors were mounted inside the pipe with only the sensing area installed flush with the pipe circumference and exposed to the soil. The diameter of the sensing area was 25 mm and 12 mm for the Scaime and Futek sensors, respectively. Scaime sensors were installed along a circular cross section at the middle of the pipe to monitor the soil pressure away from the retractable window. Futek sensors were placed around the sides of the retractable window and at distances ±19 mm from the middle of the pipe. Such arrangement allowed monitoring the changes in earth pressure in the vicinity of the retracted section and at other critical locations along the pipe circumference. It should be noted that the sizes of the different sensors were chosen such that all sensors fit inside the model tunnel (particularly the four sensors around the retractable window) and at the same time provide the accuracy needed for the expected changes in soil pressure. The locations of the sensors were chosen based on the previously conducted numerical studies (Meguid and Dang, 2009) which suggested that changes in lining load resulting from erosion voids develop mainly in the close vicinity of the introduced void. Fig. 5 shows the placement of the sensors on the tunnel lining.

2.4. Fine sand

Quartz Industrial 7030 sand was used as the backfill material. Soil characterization and direct shear tests were performed on several randomly selected samples. The density of the sand in the tank was also measured during the tests by placing small containers of

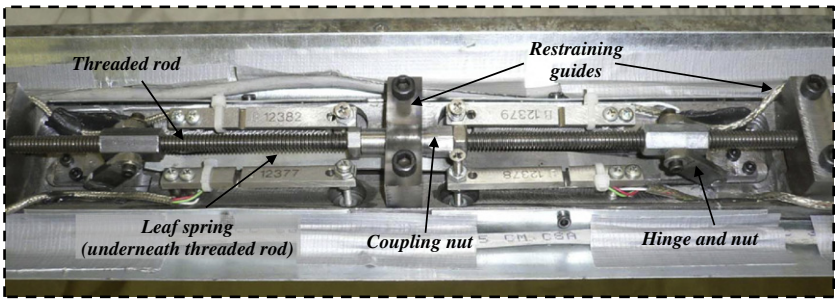

Fig. 4. Internal details of the retractable window.

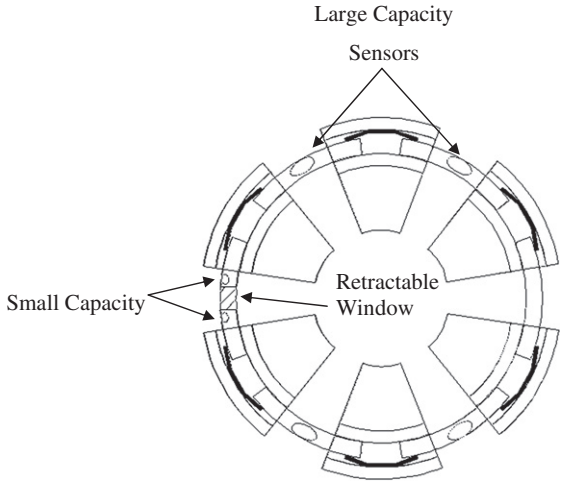

Fig. 5. Sensor placement on the tunnel lining.

Table 1
Soil properties.

Property	Value
Specific gravity	2.66
Coefficient of uniformity (C_u)	1.9
Coefficient of curvature (C_c)	0.89
Maximum dry unit weight (γ_{max})	15.7 (kN/m^3)
Minimum dry unit weight (γ_{min})	14.1 (kN/m^3)
Experimental dry unit weight (γ_d)	15 (kN/m^3)
Unified soil classification system	SP
Internal friction angle (ϕ)	39°
Cohesion (c)	0 (kPa)

known volume at different depths inside the tank. A summary of the sand properties is provided in Table 1.

3. Testing procedure

To ensure the loads cells measure the correct pressures, the entire tunnel model was subjected to a hydrostatic pressure and the readings were recorded and compared to the expected pressure values. Results indicate a linearly increasing pressure with depth. At a depth of 0.9 m below water surface, the maximum hydrostatic pressure was found to be 8.6 kPa which is consistent with the expected value of $\gamma_w\ h_w = 9.81 \times 0.9 = 8.8$ kPa.

Before testing, the exposed sensing areas were sealed using thin plastic wrap while the moving sides of the aluminum shims were covered with thin layers of silicone. This was necessary to prevent the sand penetration inside the tunnel or clogging the sensing areas. The procedure consisted of installing the tunnel under contracted condition (144 mm OD) in the tank. As the tunnel crosses the tank face, two rubber membranes having 150 mm diameter hole were slipped from inside the tank. The tunnel was expanded to its maximum diameter (150 mm) and its horizontal position was checked. Two machined plexiglass connections were installed at the extremities of the pipe to facilitate free sliding in the vertical direction (see Fig. 2). The external plexiglass connections attached to the tunnel were lifted and clamped to prevent the tunnel from resting directly on the rigid boundaries of the tank. The role of the rubber membrane was to prevent the sand leakage that could occur from the existing gap between the tunnel and the tank. To maintain the horizontal position of the tunnel while the test is running, two vertical LVDTs were attached to the plexiglass connections and connected to the data acquisition system.

A testing procedure was developed in order to ensure consistent initial conditions (i.e. sand density) throughout the conducted experiments. From the tank base up to the tunnel invert, the soil was rained in three layers 100 mm in height. Each layer was first graded to level the surface then tamped using a steel plate attached to a wooden handle. The sand placement continued up to the tunnel invert. Above the invert, the rained sand was gently pushed around the tunnel up to the crown to ensure full contact between the sand and the tunnel. At this stage, the sensors were switched on to record the earth pressure. Another layer of sand was then added to completely cover the tunnel. The remaining sand required to reach the height of 2D above the crown was placed with no tamping. The clamps holding the tunnel were removed simultaneously allowing it to slide vertically and rest on the bedding sand layer. The horizontal position of the tunnel was re-checked using the recorded readings of the vertical LVDTs attached to the plexiglass connections.

Once the initial conditions were established, the next step was to contract the tunnel to induce radial soil movement. This was done by turning a wheel connected to the threaded rod on the tunnel. The contraction was carefully monitored by LVDTs until a decrease of 2 mm in diameter was reached. The sand was allowed to settle around the tunnel and the sensor readings were allowed to stabilise before advancing to the next step. Retracting the window to simulate a local support loss was the last step of the test. Since the window could retract up to 3 mm, this action was split into two parts each representing a movement of 1.5 mm away from the sand. After each retraction, the sensor readings were recorded and the test completed. Finally, after the test, while the box was being emptied, the sand sampling cups were recovered and the sand density was measured.

3.1. Testing scheme

The experiments were conducted and repeated three times for each window position (springline, invert and haunch) with a total of nine experiments performed in this study. The developed testing procedure described above was strictly followed for each test to ensure consistent initial conditions. The results of the three tests conducted for each window position are summarized in Figs. 7–9, respectively, and discussed in the following section.

4. Results and discussion

The results of the nine tests conducted (three tests at each of the window positions shown in Fig. 6) revealed consistent changes in earth pressure experienced by the sensors located in the close vicinity of the retracted window. In all tests, no significant changes in pressure were measured by the sensors located away from the window. This was attributed to the pressure re-distribution locally around the area that experienced the contact loss. Since the other sensors did not register significant change in pressure with the retraction of the window, their data are not presented in this study. The measured results at the three tested locations are summarized in Table 2 and discussed in details below.

4.1. At the springline

Fig. 7 shows the measured changes in contact pressure (from the three conducted tests) as recorded by the sensors located in the vicinity of the retractable window versus the window movement. The pressure is normalized with respect to the initial condition. When positioned at the springline, the retraction of the

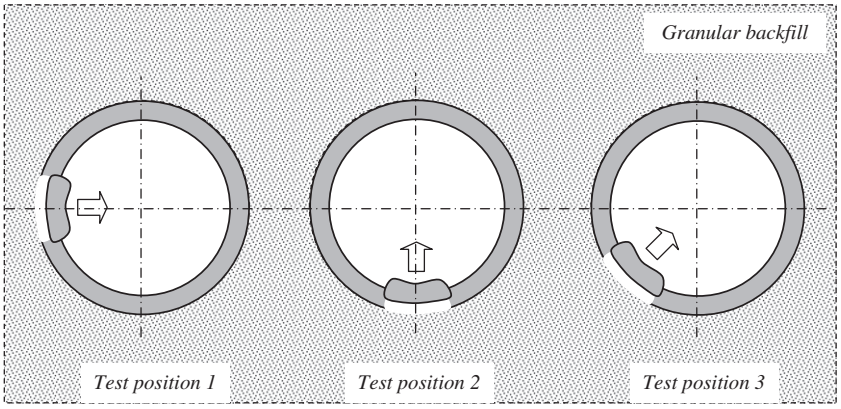

Fig. 6. Schematic of the test positions.

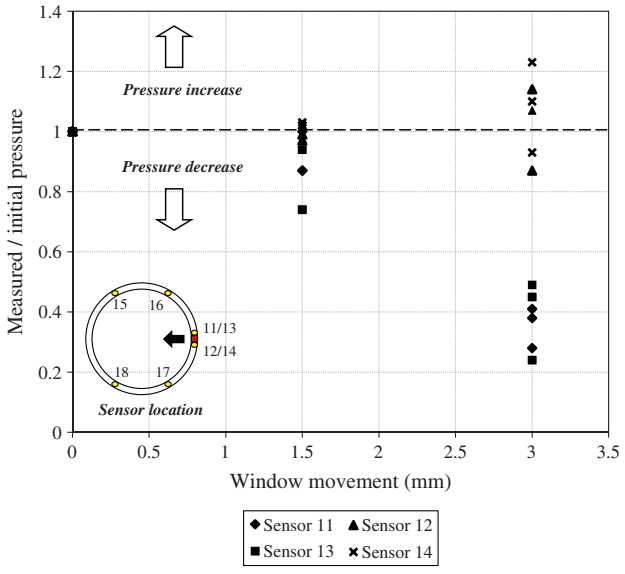

Fig. 7. Measured changes in contact pressure around the retracted window at the springline (based on the three conducted tests).

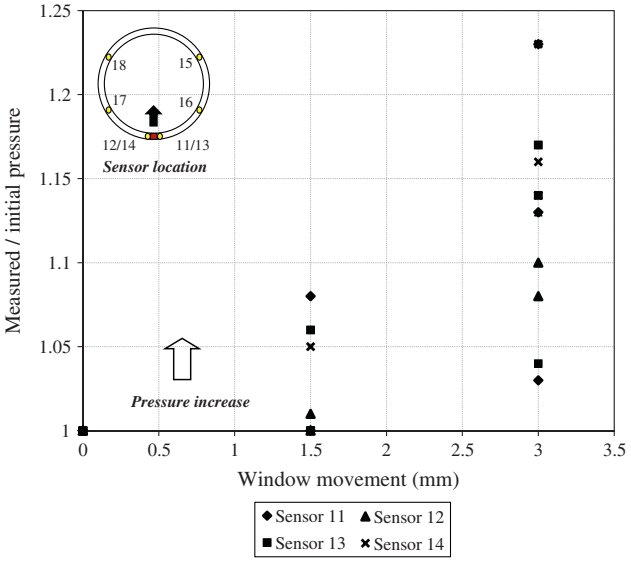

Fig. 8. Measured changes in contact pressure around the retracted window at the invert (based on the three conducted tests).

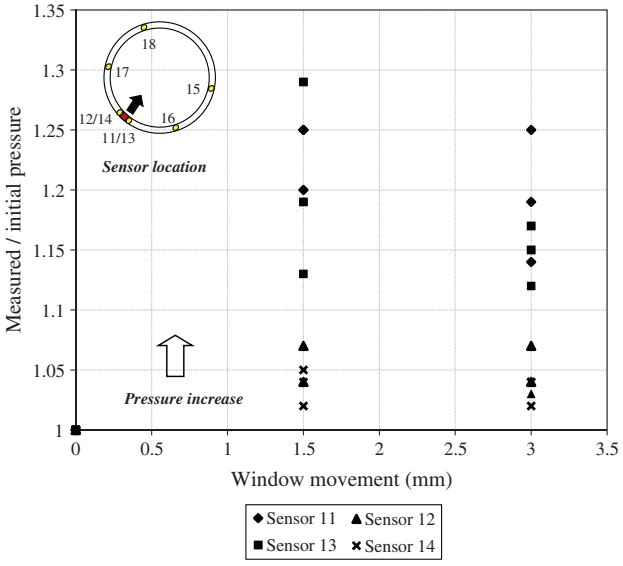

Fig. 9. Measured changes in contact pressure around the retracted window at the haunch (based on the three conducted tests).

window produced different pressure readings in the sensors located immediately above and below the window. In sensors 11 and 13 located above the window, the pressure gradually decreased as the window was retracted whereas the pressure reading in sensors 12 and 14 located below the window slightly increased. The maximum decrease in pressure of the upper sensors reached about 75% of the initial pressure when a retraction of 3 mm was induced. This behaviour can be explained by the soil movement from the area above the window into the created void leading to a release in contact pressure in the close vicinity of the upper sensors.

4.2. At the invert

Fig. 8 shows the pressure changes measured in the three conducted tests when the retracted window was located at the tunnel invert. All four sensors measured an increase in pressure with the retraction of the window. For a retraction of 1.5 mm, the maximum pressure increase reached about 7% of the initial pressure and continued to increase to about 23% of the initial pressure when the retraction reached 3 mm.

4.3. At the haunch

When the window was positioned at the bisecting 45° angle between the springling and the invert, all the pressure sensors

Table 2
Summary of the experimental Results.

Movement (mm)	% Change in pressure at sensors 11 and 13						% Change in pressure at sensors 12 and 14					
	Test 1		Test 2		Test 3		Test 1		Test 2		Test 3	
Window at springline												
1.5	0	−6	−13	−26	−13	−26	−3	+3	−1	+2	−1	+2
3.0	−72	−76	−59	−51	−62	−55	+14	+23	−13	−7	+7	+11
Window at invert												
1.5	0	0	0	0	+8	+6	+1	0	0	0	+6	+5
3.0	+13	+14	+3	+4	+23	+17	+10	+23	+8	+16	+13	+14
Window at haunch												
1.5	+25	+19	+20	+13	+25	+29	+7	+4	+4	+2	+4	+5
3.0	+28	+17	+21	+12	+14	+15	+7	+4	+4	+2	+3	+4

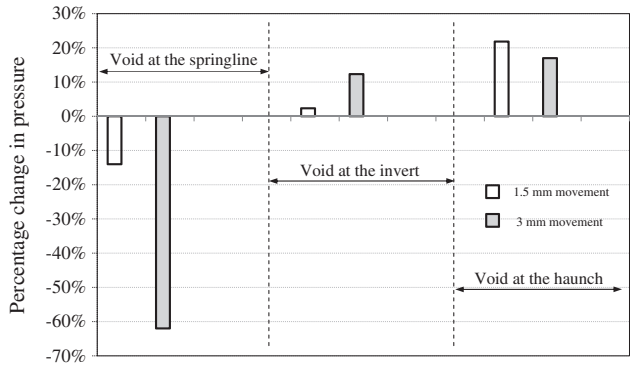

Fig. 10. Average change in pressure at the void boundary (to the right of the retracted window).

showed a pressure increase as the window was retracted. The sensors located above the window showed slightly different reactions than the sensors below. Below the window, sensors 12/14 showed a relatively small pressure increases ranging from 3% to 7% of the initial pressure. The upper sensors (sensors 11/13) recorded increase ranging from 12% to 28% as shown in Fig. 9. This behaviour is similar to that recorded at the springline with limited soil movement observed above the window. The pressure slightly decreased as the retraction increased from 1.5 mm to 3 mm.

To visualize the relative changes in contact pressure at different locations across the tunnel, the average of the pressure changes recorded at one boundary of the retracted window (sensors 11/13) are presented in Fig. 10 based on the three conducted tests at each window positions. The contract pressure generally increased in the vicinity of the area that has experienced contact loss with most significant increase when the void was introduced at the springline. This can be explained by the soil arching that developed around the retracted window leading to the re-distribution of pressure to the surrounding areas. The changes in pressure were mostly happening in the immediate vicinity of the retracted window with a maximum pressure increase of about 20% away from the window in all the conducted experiments. These findings are also consistent with the numerical investigations reported by Meguid and Dang (2009) that calculated a rapid change in lining forces at the boundaries of the erosion voids when the void was introduced at the invert and springline of an existing tunnel lining.

5. Summary and conclusions

Experimental investigations have been conducted to examine the role of local contact loss between a tunnel and the supporting soil on the earth pressure distribution on the lining. A mechanically adjustable lining has been designed to facilitate the simulation of the soil movement around the lining during construction. A retractable window 250 mm in length and 10 mm in width positioned at three different positions (springline, invert and haunch) has been used to represent the contact separation. Pressure cells installed in the close vicinity of the window were used to measure the changes in pressure due to the progressive retraction of the window. The following conclusions were reached:

(1) The introduction of the local contact loss at the springline caused pressure increase of about 25% of the initial pressure immediately below the separation zone and decrease of about 75% right above the springline.
(2) Consistent increase in pressure was observed at the invert and haunch with an increase in pressure of about 28%.
(3) Due to the small size of the retractable window no changes in pressure were measured elsewhere on the tunnel lining.

It should be noted that the above conclusions are based on limited number of experiments conducted using a reduced scale tunnel model under 1 g condition. The changes in pressure were measured at the locations of the installed sensors (around the tunnel springline, invert and haunch). Large scale experiments may assist in verifying the above findings for large diameter tunnels under full overburden pressure.

Acknowledgements

This research is supported by the Natural Sciences and Engineering Research Council of Canada (NSERC) under grant number 311971-06. The assistance of Mr. John Bartczak in building the tunnel apparatus and conducting the experiments is really appreciated.

References

Asakura, T., Kojima, Y., 2003. Tunnel maintenance in Japan. Tunnelling and Underground Space Technology 18, 161–169.
Chambon, P., Corte, J.F., 1994. Shallow tunnels in cohesionless soil: stability of tunnel face. Journal of Geotechnical Engineering 120 (7), 1148–1165.
Davis, A.G., Lim, M.K., Petersen, C.G., 2005. Rapid economical evaluation of concrete tunnel linings with impulse response and impulse radar non-destructive methods. Non-Destructive Testing and Evaluation International 38, 181–186.
Helfrich, S.C., 1997. Investigation of sewer-line failure. Journal of Performance of Constructed Facilities 42, 44.
Lee, Y., Yoo, C., 2006. Behavior of a bored tunnel adjacent to a line of load piles. Tunneling and Underground Space Technology 21 (3), 370.
MacDonald, S.E., and Zhao, J.Q. 2001. Condition assessment and rehabilitation of large sewers. In: International Conference on Underground Infrastructure Research, University of Waterloo, Ontario, pp. 361-369.
Meguid, M.A., Dang, H.K., 2009. The effect of erosion voids on existing tunnel linings. Tunnelling and Underground Space Technology 24 (3), 278–286.
Meguid, M.A., Saada, O., Nunes, M.A., Mattar, J., 2008. Physical modeling of tunnels in soft ground: a review. Tunnelling and Underground Space Technology 23 (2), 185–189.

Nomoto, T., Imamura, S., Hagiwara, T., Kusakabe, O., Fujii, N., 1999. Shield tunnel construction in centrifuge. Journal of Geotechnical and Geoenvironmental Engineering 125 (4), 289–300.

Park, S.H., Adachi, T., Kimura, M., Kishida, K., 1999. Trap door test using aluminum blocks, In: Proceedings of the 29th Symposium of Rock Mechanics. J.S.C.E., pp. 106–111.

TA, I., 1991. Report on the damaging effects of water on tunnels during their working life. Tunnelling and Underground Space Technology 6 (1), 11–76.

Talesnick, M., Baker, R., 1999. Investigation of the failure of a concrete-lined steel pipe. Geotechnical and Geological Engineering 17, 99–121.

Tan, Z., Moore, I.D. 2007. Effect of backfill erosion on moments in buried rigid pipes. In: Transportation Research Board Annual Conference, Washington DC, January 29.

Terzaghi, K.N., 1943. Theoretical Soil Mechanics, Wiley, New York.